Monthly Notices
of the
ROYAL ASTRONOMICAL SOCIETY

MNRASL **431,** L88–L92 (2013)
Advance Access publication 2013 March 7

doi:10.1093/mnrasl/slt014

Physical conditions of the gas in an ALMA [C II]-identified submillimetre galaxy at $z = 4.44$

M. T. Huynh,[1⋆] R. P. Norris,[2] K. E. K. Coppin,[3] B. H. C. Emonts,[2] R. J. Ivison,[4] N. Seymour,[2] Ian Smail,[5] V. Smolčić,[6,7,8] A. M. Swinbank,[5] W. N. Brandt,[9] S. C. Chapman,[10] H. Dannerbauer,[11] C. De Breuck,[6] T. R. Greve,[12] J. A. Hodge,[13] A. Karim,[5] K. K. Knudsen,[14] K. M. Menten,[15] P. P. van der Werf,[16] F. Walter[13] and A. Weiss[15]

[1]*International Centre for Radio Astronomy Research, M468, University of Western Australia, Crawley, WA 6009, Australia*
[2]*CSIRO Astronomy and Space Science, PO Box 76, Epping, NSW 1710, Australia*
[3]*Department of Physics, McGill University, 3600 Rue University, Montreal, QC H3A 2T8, Canada*
[4]*UK Astronomy Technology Centre, Royal Observatory, Blackford Hill, Edinburgh EH9 3HJ, UK*
[5]*Institute for Computational Cosmology, Department of Physics, Durham University, Durham DH1 3LE, UK*
[6]*European Southern Observatory, Karl-Schwarzschild-Straße 2, D-85748 Garching b. Muenchen, Germany*
[7]*Argelander Institut for Astronomy, Auf dem Hugel 71, D-53121 Bonn, Germany*
[8]*Physics Department, University of Zagreb, Bijenička cesta 32, HR-10002 Zagreb, Croatia*
[9]*Department of Astronomy and Astrophysics, Pennsylvania State University, 525 Davey Lab, University Park, PA 16802, USA*
[10]*Institute of Astronomy, University of Cambridge, Madingley Road, Cambridge CB3 0HA, UK*
[11]*Institut für Astrophysik, Universität Wien, Türkenschanzstraße 17, A-1180 Wien, Austria*
[12]*Department of Physics and Astronomy, University College London, Gower Street, London WC1E 6BT, UK*
[13]*Max-Planck Institute for Astronomy, Königstuhl 17, D-69117 Heidelberg, Germany*
[14]*Department of Earth and Space Sciences, Chalmers University of Technology, Onsala Space Observatory, SE-43992 Onsala, Sweden*
[15]*Max-Planck-Institut für Radioastronomie, Aus dem Hügel 69, D-53121 Bonn, Germany*
[16]*Leiden Observatory, Leiden University, PO Box 9513, NL-2300 RA Leiden, the Netherlands*

Accepted 2013 January 30. Received 2013 January 29; in original form 2012 December 10

ABSTRACT

We present ^{12}CO(2–1) observations of the submillimetre galaxy ALESS65.1 performed with the Australia Telescope Compact Array (ATCA) at 42.3 GHz. A previous Atacama Large Millimeter Array study of submillimetre galaxies (SMGs) in the Extended *Chandra* Deep Field South detected [C II] 157.74 μm emission from this galaxy at a redshift of $z = 4.44$. No ^{12}CO(2–1) emission was detected but we derive a firm upper limit to the cold gas mass in ALESS65.1 of $M_{\rm gas} < 1.7 \times 10^{10}\,{\rm M}_{\odot}$. The estimated gas depletion time-scale is <50 Myr, which is similar to other high-redshift SMGs, and consistent with $z > 4$ SMGs being the likely progenitors of massive red-and-dead galaxies at $z > 2$. The ratio of the [C II], ^{12}CO and far-infrared luminosities implies a strong far-ultraviolet field of $G_0 \gtrsim 10^3$, as seen in Galactic star-forming regions or local ultraluminous infrared galaxies (ULIRGs). The observed $L_{\rm [C\,II]}/L_{\rm FIR} = 2.3 \times 10^{-3}$ is high compared to local ULIRGs and, combined with $L_{\rm [C\,II]}/L_{\rm CO} \gtrsim 2700$, it is consistent with ALESS65.1 either having an extended (several kpc) [C II] emitting region or lower than solar metallicity.

Key words: galaxies: evolution – galaxies: formation.

1 INTRODUCTION

Submillimetre galaxies (SMGs) are ultraluminous, dusty starbursting systems with extreme star formation rates (SFRs) of 100–1000 $\rm M_{\odot}\ yr^{-1}$ (e.g. Blain et al. 2002). These SMGs have typical redshifts of $z \sim 2$–3 (e.g. Chapman et al. 2005; Wardlow et al. 2011; Smolčić et al. 2012; Yun et al. 2012), but an increasing number of higher redshift SMGs are being found. The $z > 4$ SMGs represent candidates for the most intense star formation phase of the massive red galaxies seen at $z > 2$ (Cimatti et al. 2008; Marchesini et al. 2010). This high-redshift tail of the SMG distribution was long underrepresented in SMG redshift surveys, mostly because they lie below the sensitivity limits of the radio interferometer surveys used

⋆E-mail: minh.huynh@uwa.edu.au

to identify SMGs. However, in the last few years, over a dozen of these sources have been reported (Capak et al. 2008, 2011; Coppin et al. 2009; Daddi et al. 2009a,b; Carilli et al. 2010, 2011; Knudsen et al. 2010; Riechers et al. 2010; Cox et al. 2011; Smolčić et al. 2011; Combes et al. 2012; Walter et al. 2012), and recent Atacama Large Millimeter Array (ALMA) redshift surveys have doubled these numbers (Vieira et al. submitted; Weiss et al. submitted). Detailed studies of the star formation and gas content in these $z > 4$ SMGs are still rare, but are needed to provide a unique insight into the earliest phases of the growth of massive elliptical galaxies.

The most accessible tracer of cold gas in galaxies is ^{12}CO, which has been observed extensively in SMGs (e.g. Greve et al. 2005; Tacconi et al. 2006; Bothwell et al. 2013). Detections of ^{12}CO in $z > 4$ SMGs have shown that they are gas-rich systems with sufficient reservoirs ($M_{\rm gas} > 10^{10}\,{\rm M}_{\odot}$) to sustain the extreme SFRs of $\sim$1000 $\rm M_{\odot}\ yr^{-1}$ for only short time-scales (tens of Myr) (Coppin et al. 2010; Riechers et al. 2010), unless the gas is replenished. This is consistent with high-redshift SMGs being the progenitors of the luminous red galaxies seen at $z > 2$.

The $^2P_{3/2} - {}^2P_{1/2}$ fine structure line of singly ionized carbon at 157.74 μm (hereafter [C II]) has emerged as a powerful alternative line for studying the interstellar medium (ISM) in high-redshift sources. It can represent up to 1 per cent of the bolometric luminosity of star-forming galaxies (e.g. Crawford et al. 1985; Stacey et al. 1991). This line emission arises mainly from the photodissociation regions (PDRs) that form at the edges of molecular clouds illuminated by the UV photons of young-massive stars, but a significant contribution can also come from H II regions and the more diffuse warm ISM (Madden et al. 1993; Heiles 1994). The [C II] line therefore provides an important probe of the gas content and star formation processes in a galaxy.

A recent ALMA Cycle 0 study of 126 submillimetre sources located in the LABOCA Extended *Chandra* Deep Field South (LESS; Weiß et al. 2009; Karim et al. 2013; Hodge et al. 2013, submitted) resulted in the serendipitous identification of [C II] line emission from two SMGs (Swinbank et al. 2012, hereafter S12). The average [C II]/far-infrared (FIR) luminosity ratio of these two SMGs is $\sim$0.0012 ± 0.0004, roughly ten times higher than that observed in local ultraluminous infrared galaxies (ULIRGs), which has been interpreted as evidence that their gas reservoirs are more extended (S12). The large extent of SMGs is supported by other observations, such as extended radio morphologies (e.g. Chapman et al. 2004; Biggs & Ivison 2008), extended Hα morphologies (e.g. Swinbank et al. 2006), large ^{12}CO(1–0) sizes (Ivison et al. 2010a, 2011; Hodge et al. 2012; Thomson et al. 2012), lack of silicate absorption in mid-IR spectra (Menéndez-Delmestre et al. 2009) and less reddened broad-band mid-IR colours (Hainline et al. 2009). High [C II]/FIR ratios (Stacey et al. 2010; Ivison et al. 2010b; S12) add to this mounting evidence that star formation in SMGs takes place in a region larger than the compact nuclear starbursts of local ULIRGs.

In this Letter, we present ^{12}CO(2–1) observations of one of the ALMA-detected SMGs, ALESS J033252.26−273526.3 (hereafter ALESS65.1). We adopt the standard Λ cold dark matter cosmological parameters of $\Omega_{\rm M} = 0.27$, $\Omega_{\Lambda} = 0.73$ and a Hubble constant of 71 $\rm km\ s^{-1}\ Mpc^{-1}$ throughout this Letter.

2 OBSERVATIONS AND RESULTS

The ^{12}CO(2–1) line ($\nu_{\rm rest} = 230.538$ GHz) in ALESS65.1 [RA (J2000) = 03 32 52.26, Dec. (J2000) = −27 35 26.3] (S12) was observed over a period of four consecutive nights, 2012 August 9–12 , with the ATCA, using the Compact Array Broadband Backend (CABB). The array was in the most compact five-antenna configuration, H75, which has a maximum baseline of 89 m and two antennas set along a northern spur. The hybrid configuration allows good (u, v) coverage to be obtained for integrations less than the full 12 h synthesis. We centred the 7 mm IF1 receiver on 42.343 GHz, the expected frequency of the ^{12}CO(2–1) line emission given the [C II] redshift of $z = 4.4445$ derived by S12. The 2 GHz wide bandwidth of CABB results in a frequency coverage of 41.3 to 43.3 GHz, covering ^{12}CO(2–1) emission between $z = 4.32$ and 4.58. The weather was good to average, with rms atmospheric path length variations of 100–400 μm throughout the run, as measured on the 230 m baseline ATCA Seeing Monitor (Middelberg, Sault & Kesteven 2006). The system temperature was 140–250 K throughout the four nights. Weather and atmospheric conditions can induce temporal fluctuations across the wide CABB band, so, following Emonts et al. (2011), a bandpass calibration scan was acquired at the beginning, middle and end of each 8 h night. Phase and amplitude calibration information was acquired with 2 min scans on PKS 0346−279 every 10 min and pointing checks performed on the same source every hour. Flux density calibration was performed on Uranus at the beginning of the nights, when it was at an elevation of roughly 55°. The uncertainty in the flux density calibration using the standard MIRIAD model of Uranus is estimated to be 30 per cent (Emonts et al. 2011).

The data were calibrated, mapped and analysed using the standard MIRIAD (Sault & Killeen 1999) and KARMA (Gooch 1996) packages. The synthesized beam from natural weighting is 14.0 × 9.9 arcsec. A total of about 20 h on-source integration time was obtained over the 4 × 8 h nights. ALESS65.1 was not detected in the 42.3 GHz continuum map from the full CABB band, which achieves an rms noise level of 11 $\rm \mu Jy\ beam^{-1}$.

The resultant channel noise in the 1 MHz (7.1 $\rm km\ s^{-1}$) wide spectrum is $\sim$0.43 $\rm mJy\ beam^{-1}$, consistent with other comparable 7 mm ATCA/CABB surveys (e.g. Coppin et al. 2010; Emonts et al. 2011). The visibilities were resampled to velocity resolutions of 50, 100 and 200 $\rm km\ s^{-1}$ and each cube was examined for an emission line near the ALMA position. An $\sim 4\sigma$ spike at the position of ALESS65.1 and an offset from the [C II] emission by $\sim$280 $\rm km\ s^{-1}$ were examined in detail. It was deemed a noise spike because it is only present in one channel in all three binned images and is present only in the last night of data when each night is imaged separately. We flag the spike (20 native channels) in the last night of data and recombined all four nights of data to derive the final spectra. The spectra at the source position in the 100 and 200 $\rm km\ s^{-1}$ binned cubes (Fig. 1) have an rms of 0.11 and 0.08 $\rm mJy\ beam^{-1}$, respectively. Assuming a line FWHM identical to the [C II] emission line (470 $\rm km\ s^{-1}$; S12) and adopting a 3σ limit, the ^{12}CO(2–1) line intensity of ALESS65.1 is $I_{\rm CO(2-1)} < 0.11$ Jy $\rm km\ s^{-1}$.

3 DISCUSSION

The observed and derived properties of ALESS65.1 are summarized in Table 1. To estimate the cold molecular gas content in ALESS65.1, we calculate upper limits to the line luminosity and total cold gas (H_2 + He) mass from the CO(2–1) flux density limit. Following Solomon & Vanden Bout (2005), the line luminosity upper limit is $L'_{\rm CO(2-1)} < 2.2 \times 10^{10}$ K $\rm km\ s^{-1}\ pc^2$. If we assume that the gas is thermalized (i.e. intrinsic brightness temperature and line luminosities are independent of J transition), so $L'_{\rm CO(2-1)} = L'_{\rm CO(1-0)}$, and a CO-to-$H_2$ conversion factor $\alpha = 0.8\,{\rm M}_{\odot}$ (K $\rm km\ s^{-1}\ pc^2)^{-1}$, which is appropriate for ULIRGs (e.g. Downes & Solomon 1998,

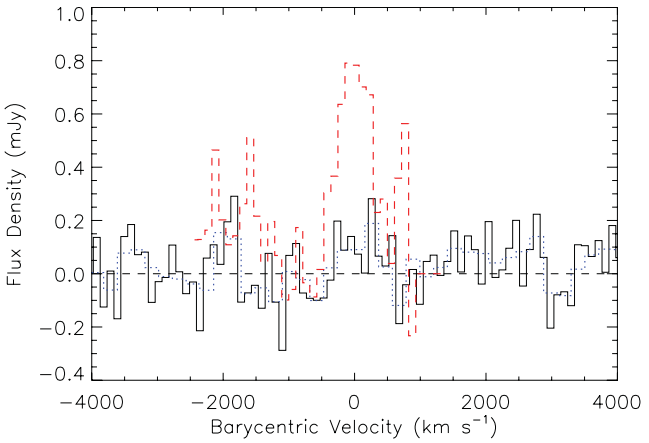

Figure 1. ^{12}CO(2–1) spectrum of ALESS65.1 binned into 100 km s^{-1} channels and extracted at the ALMA position. The red dashed line shows the ALMA [C II] spectrum from S12, binned to a similar channel width (120 km s^{-1}) and with the flux density divided by 15 for clarity. The blue dotted line shows the spectrum binned into 200 km s^{-1} for maximum sensitivity. We conclude that no line was detected to a 3σ limit of 0.24 mJy beam^{-1} per 200 km s^{-1} channel.

Table 1. Observed and derived properties of ALESS65.1.

Parameter	Value	Reference
$z_{\rm [C\,II]}$	4.4445 ± 0.0005	S12
$I_{\rm [C\,II]}$	5.4 ± 0.7 Jy km s^{-1}	S12
FWHM$_{\rm [C\,II]}$	470 ± 35 km s^{-1}	S12
$L_{\rm [C\,II]}$	$(3.2 \pm 0.4) \times 10^9$ L$_\odot$	S12
$L_{\rm FIR}$ [a]	$(1.38 \pm 0.28) \times 10^{12}$ L$_\odot$	S12
$I_{\rm CO(2-1)}$	<0.11 Jy km s^{-1} (3σ)	This Letter
$M_{\rm gas}$	$< 1.7 \times 10^{10}$ M$_\odot$ (3σ)	This Letter
$L_{\rm CO(2-1)}$	$< 8.5 \times 10^6$ L$_\odot$ (3σ)	This Letter
$L'_{\rm CO(2-1)}$	$< 2.2 \times 10^{10}$ K km s^{-1} pc^2	This Letter

[a]Converted from $L_{\rm IR}$(8–1000 μm) using $L_{\rm FIR}$(42–122 μm) = $L_{\rm IR}$/1.45 (Stacey et al. 2010; De Breuck et al. 2011).

but see Bothwell et al. 2013), the upper limit on the total cold gas mass is $M_{\rm gas} < 1.7 \times 10^{10}$ M$_\odot$. This is consistent with the gas mass found in other $z > 4$ SMGs (Schinnerer et al. 2008; Daddi et al. 2009a; Coppin et al. 2010; Walter et al. 2012) and the typical [C II]/$M_{\rm gas}$ ratio at high redshift (S12).

The total baryonic mass of ALESS65.1 can be derived by combining the gas and stellar mass estimates for the system. The stellar mass of the system was estimated from the rest-frame absolute H-band magnitude to be $M_* \sim 9 \times 10^{10}$ M$_\odot$ (S12), so the gas fraction is modest with $M_{\rm gas}/M_* \lesssim 0.2$. The total baryonic mass $M_{\rm bary} = M_{\rm gas} + M_*$ is ∼9–11 × 10^{10} M$_\odot$. This is consistent with the dynamical mass for the system, based on the [C II] linewidths and spatial extent, of $M_{\rm dyn} \sin^2(i) \sim (3.4 \pm 1.8) \times 10^{10}$ M$_\odot$ (S12).

ALESS65.1 is detected in the 870 μm continuum by ALMA and weakly detected in the FIR by *Herschel* (S12). A fit to the IR Spectral Energy Distribution (SED) resulted in a rest-frame IR (8–1000 μm) luminosity $L_{\rm IR} = (2.0 \pm 0.4) \times 10^{12}$ L$_\odot$ (S12), which corresponds to an SFR of ∼340 M$_\odot$ yr^{-1} using the conversion of Kennicutt (1998). The gas depletion time-scale $\tau = M_{\rm gas}/{\rm SFR} <$ 50 Myr is similar to the gas depletion rates of other high-redshift SMGs (Schinnerer et al. 2008; Coppin et al. 2010). This short time-scale provides further evidence that $z > 4$ SMGs have the gas consumption time-scales necessary to be the progenitors of red-and-dead 'ellipticals' at $z > 2$.

Next, we examine the physical conditions of the gas in ALESS65.1 using the [C II] detection and ^{12}CO(2–1) limit. The $L_{\rm [C\,II]}/L_{\rm FIR}$ versus $L_{\rm CO(1-0)}/L_{\rm FIR}$ diagram is a powerful diagnostic as these two ratios are sensitive to gas density n and the incident far-ultraviolet (FUV) flux G_0 (Stacey et al. 1991). Fig. 2 shows ALESS65.1 compared with other low- and high-redshift galaxies, and solar metallically PDR model curves (Kaufman et al. 1999). This diagram can be used to roughly estimate both n and G_0 for a galaxy, but there are some caveats, as outlined in De Breuck et al. (2011). These are: (i) the ^{12}CO luminosity is that of the ground state rotational line, (ii) [C II] emission from the diffuse ionized medium and cosmic ray-heated gas is assumed to be small compared to that from PDRs and (iii) AGN and their related X-ray dissociation regions are assumed to not contribute significantly to the FIR and [C II] luminosity. To be consistent with both De Breuck et al. (2011) and Stacey et al. (2010) in Fig. 2, we assume $L_{\rm CO(2-1)}/L_{\rm CO(1-0)} = 7.2$, which is 90 per cent of its value if the gas was fully thermalized and optically thick. Cosmic ray rates are greater in starbursts compared to normal galaxies but this does not seem to result in higher [C II]/CO ratios, so cosmic ray ionization does not appear to dominate the [C II]/CO ratio (De Breuck et al. 2011), at least for local galaxies. ALESS65.1 is not detected in the 250 ks *Chandra* X-Ray observations of this region (Lehmer et al. 2005), so it is not a luminous QSO ($L_{\rm 3-44keV} \lesssim 2$–$3 \times 10^{44}$ erg s^{-1}, for $N_{\rm H} = 0$–$10^{23.5}$ cm^{-2}). The maximum likely AGN contribution to the FIR luminosity is estimated from a multicomponent (AGN and starburst) fit to the FIR using DECOMPIR software (Mullaney et al. 2011) and following the method described by Seymour et al. (2012). We use the 24 μm flux density upper limit to constrain the short wavelength part of the IR SED and find that the AGN contribution to the total FIR luminosity is $\lesssim$10 per cent. ALESS65.1 therefore appears to be dominated by star formation processes and the AGN contribution to [C II] and $L_{\rm FIR}$ is minimal.

In examining the PDR physical conditions, we multiply the ^{12}CO(2–1) flux by a factor of 2 to account for the line being optically thick, and hence only the ^{12}CO emission coming from the illuminated PDR side is seen (Kaufman et al. 1999; Hailey-Dunsheath et al. 2010). We also multiply the [C II] flux by a factor of 0.7 to remove non-PDR contributions (e.g. Hailey-Dunsheath et al. 2010; Stacey et al. 2010). The ^{12}CO geometry correction applies to all galaxies in Fig. 2, and so does not affect the relative position of ALESS65.1 on the diagram compared to other galaxies. Using the Kaufman et al. (1999) models, we find ALESS65.1 has $G_0 \sim 10^3$ and $n \lesssim 10^5$ cm^{-3} (Fig. 2). Such an FUV radiation field is on the high end of those seen in low-redshift normal galaxies, but it is consistent with the strong FUV fields seen in local starbursts, nearby ULIRGs, and some $z > 1$ galaxies. This limit on G_0 and n implies a PDR temperature $\gtrsim$300 K (Kaufman et al. 1999). Using equation 1 from Hailey-Dunsheath et al. (2010), we estimate the atomic gas associated with the PDR to be greater than 3×10^9 M$_\odot$. We note that this atomic mass estimate is very uncertain, and it is highly dependent on n. The atomic gas mass $M_a \sim 2.9 \times 10^9 + (3.2 \times 10^{12}/n)$, so for $n = 10^3$ cm^{-3} the atomic mass would be ∼6 × 10^9 M$_\odot$.

ALESS65.1 and the other two $z > 4$ SMGs shown in Fig. 2, LESS J033229.4 (De Breuck et al. 2011) and HDF850.1 (Walter et al. 2012), have a similar FUV radiation field, G_0, to local starbursts, but have much higher FIR luminosity, leading to suggestions that they are scaled-up versions of local starbursts. For a given $L_{\rm FIR}$, the size of the emission region will increase for smaller G_0. Following Stacey et al. (2010), we scale up from M82 using two laws from

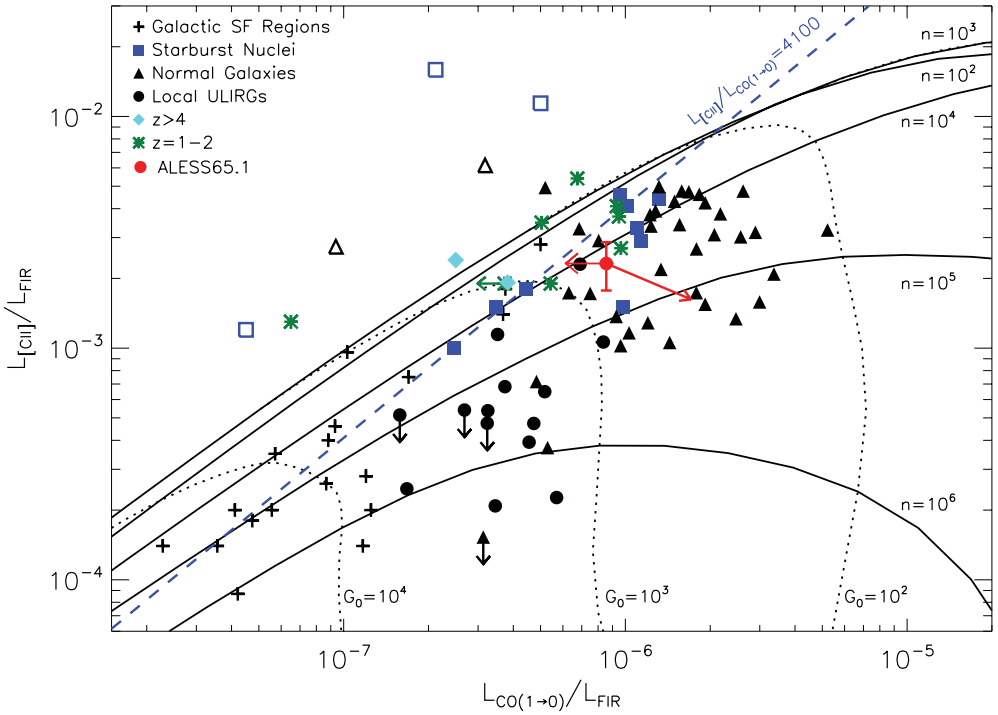

Figure 2. $L_{[\mathrm{C\,II}]}/L_{\mathrm{FIR}}$ versus $L_{\mathrm{CO(1–0)}}/L_{\mathrm{FIR}}$ for ALESS65.1 (red point with upper limit on $L_{\mathrm{CO(1–0)}}/L_{\mathrm{FIR}}$) compared with Galactic star-forming regions, starburst nuclei, normal galaxies, local ULIRGs and high-redshift ($z > 1$) sources. The empty symbols indicate low-metallicity sources, which lie at high $L_{[\mathrm{C\,II}]}/L_{\mathrm{CO(1–0)}}$. The black lines represent the solar metallicity PDR model calculations for gas density (n) and FUV field strength (G_0) from Kaufman et al. (1999). This figure is adapted from Stacey et al. (2010) with additional data from De Breuck et al. (2011) and Walter et al. (2012). ALESS65.1 has a higher $L_{[\mathrm{C\,II}]}/L_{\mathrm{FIR}}$ ratio than that found in local ULIRGs, similar to the other two $z > 4$ SMGs, but its $L_{[\mathrm{C\,II}]}/L_{\mathrm{CO}}$ ratio is similar to local starbursts and other $z > 1$ sources.

Wolfire, Tielens & Hollenbach (1990) to constrain the size: $G_0 \propto \lambda L_{\mathrm{FIR}}/D^3$ if the mean free path of a UV photon λ is small and $G_0 \propto L_{\mathrm{FIR}}/D^2$ if the mean free path of a UV photon is large. Applying these relations and using $G_0 = 10^3$ for ALESS65.1 yield a diameter of 1.1–2.1 kpc. This is consistent with the marginally resolved [C II] data which show that ALESS65.1 has a possible extent of 3.3 ± 1.7 kpc (S12). The same scaling relation applied to HDF850.1 results in a diameter of 1.8–4.6 kpc, which is consistent with the observed 5.7 ± 1.9 kpc extent of the [C II] emission region (Walter et al. 2012). Similarly, LESS J033229.4 has an extent of ∼4 kpc (Coppin et al. 2010; De Breuck et al. 2011). Thus, the starburst in all three $z > 4$ SMGs appears to be extended over galactic scales.

Local starbursts and Galactic OB star-forming regions lie on a line with [C II]/CO luminosity ratios of about 4100 in Fig. 2. Higher [C II]/CO ratios can also be found in low-metallicity systems, such as 30 Doradus in the Large Magellanic Cloud, where the size of the [C II] emitting envelope of the cloud (relative to the CO emitting core) is much larger than in more metal-rich systems (Stacey et al. 1991). Metallicity may also affect the [C II]/CO ratios of the highest redshift galaxies. For example, LESS J033229.4 at $z = 4.76$ has a very high [C II]/CO ratio of $\approx 10^4$ and was initially thought to have sub-solar metallicity (De Breuck et al. 2011), but more recent [N II] observations suggest that the metallicity of this galaxy is solar (Nagao et al. 2012). ALESS65.1 has $L_{[\mathrm{C\,II}]}/L_{\mathrm{CO}} \gtrsim 2700$, which is consistent with low metallicity, but it has an extent of several kpc so the enhanced [C II] emission is more likely to be due to the extended star-forming region. An extended (or less-dense) ISM would have an increased fraction of UV photons available to ionize and excite gas, increasing the relative intensity of fine structure lines (e.g. Graciá-Carpio et al. 2011).

We have assumed a single-phase ISM in this work. Multiphase ISMs are commonly required to explain the ^{12}CO line ratios observed in local galaxies (e.g. Guesten et al. 1993; Ward et al. 2003). In some cases a single-component ISM is unable to explain the ^{12}CO-excitation ladder (or spectral line energy distribution) observed in high-redshift SMGs (Carilli et al. 2010; Harris et al. 2010; Danielson et al. 2011). These studies found that the ISM in such sources is best described by a warm compact component surrounded by a cooler more extended one. Support for such a multicomponent geometry in high-redshift sources has recently been found in the spatially resolved ^{12}CO study of the gravitationally magnified submillimetre galaxy SMM J2135−0102 (Danielson et al. 2011; Swinbank et al. 2011). Future higher resolution continuum and line studies with ALMA may uncover similar evidence in ALESS65.1, but the current data provide no direct evidence.

4 CONCLUSION

We have observed ALESS65.1 for 20 h to search for ^{12}CO(2–1) emission in this $z = 4.44$ SMG. We detect no ^{12}CO(2–1) emission in a spectrum reaching an rms sensitivity of 0.08 mJy beam^{-1} per 200 km s^{-1} channel.

Adopting the FWHM from the ALMA detection of [C II] in ALESS65.1, we estimate a 3σ limit to the ^{12}CO(2–1) luminosity of $L_{\mathrm{CO(2–1)}} < 8.5 \times 10^6\,\mathrm{L}_\odot$ and a cold gas mass upper limit of $M_{\mathrm{gas}} < 1.7 \times 10^{10}\,\mathrm{M}_\odot$. This implies a gas depletion time-scale in ALESS65.1 of <50 Myr, comparable to other $z > 4$ SMGs and consistent with this high-redshift population being the progenitors of $z > 2$ red-and-dead galaxies.

We examine the physical conditions of the gas in ALESS65.1 using the $L_{[\mathrm{C\,II}]}/L_{\mathrm{FIR}}$ versus $L_{\mathrm{CO(1-0)}}/L_{\mathrm{FIR}}$ diagram. We find that ALESS65.1 has a strong FUV field comparable to local starbursts. The observed [C II] to FIR ratio, $L_{[\mathrm{C\,II}]}/L_{\mathrm{FIR}} = 2.3 \times 10^{-3}$, is high compared to local ULIRGs (as noted by S12). Combined with $L_{[\mathrm{C\,II}]}/L_{\mathrm{CO}} \gtrsim 2700$, this high [C II] to FIR ratio is consistent with ALESS65.1 having more extended regions of intense star formation than local ULIRGs. A possible, but less likely, scenario is that ALESS65.1 has low-metallicity gas.

Measurements of [C II] and ^{12}CO of a larger sample are needed to confirm whether $z > 4$ starbursts have enhanced [C II] emission compared to local galaxies, and whether this is because of metallicity effects, the relative size of PDR regions, a combination of the two or other effects. Future surveys by ALMA will shed further light on the physical conditions of the gas in star-forming galaxies in the early Universe.

ACKNOWLEDGEMENTS

AK and IRS acknowledge support from the STFC and IRS also acknowledges support from the Leverhulme Trust. TRG acknowledges support from an STFC Advanced Fellowship. KC acknowledges support from the endowment of the Lorne Trottier Chair in Astrophysics and Cosmology at McGill and the Natural Science and Engineering Research Council of Canada (NSERC). NS is the recipient of an Australian Research Council Future Fellowship. KK thanks the Swedish Research Council for support. The Australia Telescope is funded by the Commonwealth of Australia for operation as a National Facility managed by CSIRO. This Letter makes use of ALMA data from the project ADS/JAO.ALMA#2011.1.00294.S. ALMA is a partnership of ESO (representing its member states), NSF (USA) and NINS (Japan), together with NRC (Canada) and NSC and ASIAA (Taiwan), in cooperation with the Republic of Chile. The Joint ALMA Observatory is operated by ESO, AUI/NRAO and NAOJ.

REFERENCES

Biggs A. D., Ivison R. J., 2008, MNRAS, 385, 893
Blain A. W., Smail I., Ivison R. J., Kneib J.-P., Frayer D. T., 2002, Phys. Rep., 369, 111
Bothwell M. S. et al., 2013, MNRAS, 429, 3047
Capak P. et al., 2008, ApJ, 681, L53
Capak P. L. et al., 2011, Nat, 470, 233
Carilli C. L. et al., 2010, ApJ, 714, 1407
Carilli C. L., Hodge J., Walter F., Riechers D., Daddi E., Dannerbauer H., Morrison G. E., 2011, ApJ, 739, L33
Chapman S. C., Smail I., Windhorst R., Muxlow T., Ivison R. J., 2004, ApJ, 611, 732
Chapman S. C., Blain A. W., Smail I., Ivison R. J., 2005, ApJ, 622, 772
Cimatti A. et al., 2008, A&A, 482, 21
Combes F. et al., 2012, A&A, 538, L4
Coppin K. E. K. et al., 2009, MNRAS, 395, 1905
Coppin K. E. K. et al., 2010, MNRAS, 407, L103
Cox P. et al., 2011, ApJ, 740, 63
Crawford M. K., Genzel R., Townes C. H., Watson D. M., 1985, ApJ, 291, 755
Daddi E., Dannerbauer H., Krips M., Walter F., Dickinson M., Elbaz D., Morrison G. E., 2009a, ApJ, 695, L176
Daddi E. et al., 2009b, ApJ, 694, 1517
Danielson A. L. R. et al., 2011, MNRAS, 410, 1687
De Breuck C., Maiolino R., Caselli P., Coppin K., Hailey-Dunsheath S., Nagao T., 2011, A&A, 530, L8
Downes D., Solomon P. M., 1998, ApJ, 507, 615
Emonts B. H. C. et al., 2011, MNRAS, 415, 655
Gooch R., 1996, in Jacoby G. H., Barnes J., eds, ASP Conf. Ser. Vol. 101, Astronomical Data Analysis Software and Systems V, Astron. Soc. Pac., San Francisco, p. 80
Graciá-Carpio J. et al., 2011, ApJ, 728, L7
Greve T. R. et al., 2005, MNRAS, 359, 1165
Guesten R., Serabyn E., Kasemann C., Schinckel A., Schneider G., Schulz A., Young K., 1993, ApJ, 402, 537
Hailey-Dunsheath S., Nikola T., Stacey G. J., Oberst T. E., Parshley S. C., Benford D. J., Staguhn J. G., Tucker C. E., 2010, ApJ, 714, L162
Hainline L. J., Blain A. W., Smail I., Frayer D. T., Chapman S. C., Ivison R. J., Alexander D. M., 2009, ApJ, 699, 1610
Harris A. I., Baker A. J., Zonak S. G., Sharon C. E., Genzel R., Rauch K., Watts G., Creager R., 2010, ApJ, 723, 1139
Heiles C., 1994, ApJ, 436, 720
Hodge J. A., Carilli C. L., Walter F., de Blok W. J. G., Riechers D., Daddi E., Lentati L., 2012, ApJ, 760, 11
Hodge J. A. et al., 2013, submitted
Ivison R. J., Smail I., Papadopoulos P. P., Wold I., Richard J., Swinbank A. M., Kneib J.-P., Owen F. N., 2010a, MNRAS, 404, 198
Ivison R. J. et al., 2010b, A&A, 518, L35
Ivison R. J., Papadopoulos P. P., Smail I., Greve T. R., Thomson A. P., Xilouris E. M., Chapman S. C., 2011, MNRAS, 412, 1913
Karim A. et al., 2013, MNRAS, arXiv:1210.0249
Kaufman M. J., Wolfire M. G., Hollenbach D. J., Luhman M. L., 1999, ApJ, 527, 795
Kennicutt R. C. Jr, 1998, ARA&A, 36, 189
Knudsen K. K., Kneib J.-P., Richard J., Petitpas G., Egami E., 2010, ApJ, 709, 210
Lehmer B. D. et al., 2005, ApJS, 161, 21
Madden S. C., Geis N., Genzel R., Herrmann F., Jackson J., Poglitsch A., Stacey G. J., Townes C. H., 1993, ApJ, 407, 579
Marchesini D. et al., 2010, ApJ, 725, 1277
Menéndez-Delmestre K. et al., 2009, ApJ, 699, 667
Middelberg E., Sault R. J., Kesteven M. J., 2006, PASA, 23, 147
Mullaney J. R., Alexander D. M., Goulding A. D., Hickox R. C., 2011, MNRAS, 414, 1082
Nagao T., Maiolino R., De Breuck C., Caselli P., Hatsukade B., Saigo K., 2012, A&A, 542, L34
Riechers D. A. et al., 2010, ApJ, 720, L131
Sault R. J., Killeen N. E. B., 1999, MIRIAD User's Guide. Australia Telescope National Facility, Sydney, Australia
Schinnerer E. et al., 2008, ApJ, 689, L5
Seymour N. et al., 2012, ApJ, 755, 146
Smolčić V. et al., 2011, ApJ, 731, L27
Smolčić V. et al., 2012, ApJS, 200, 10
Solomon P. M., Vanden Bout P. A., 2005, ARA&A, 43, 677
Stacey G. J., Geis N., Genzel R., Lugten J. B., Poglitsch A., Sternberg A., Townes C. H., 1991, ApJ, 373, 423
Stacey G. J., Hailey-Dunsheath S., Ferkinhoff C., Nikola T., Parshley S. C., Benford D. J., Staguhn J. G., Fiolet N., 2010, ApJ, 724, 957
Swinbank A. M., Chapman S. C., Smail I., Lindner C., Borys C., Blain A. W., Ivison R. J., Lewis G. F., 2006, MNRAS, 371, 465
Swinbank A. M. et al., 2011, ApJ, 742, 11
Swinbank A. M. et al., 2012, MNRAS, 427, 1066 (S12)
Tacconi L. J. et al., 2006, ApJ, 640, 228
Thomson A. P. et al., 2012, MNRAS, 425, 2203
Vieira J. et al., 2013, submitted
Walter F. et al., 2012, Nat, 486, 233
Ward J. S., Zmuidzinas J., Harris A. I., Isaak K. G., 2003, ApJ, 587, 171
Wardlow J. L. et al., 2011, MNRAS, 415, 1479
Weiß A. et al., 2009, ApJ, 707, 1201
Weiss A. et al., 2013, submitted
Wolfire M. G., Tielens A. G. G. M., Hollenbach D., 1990, ApJ, 358, 116
Yun M. S. et al., 2012, MNRAS, 420, 957

This paper has been typeset from a TEX/LATEX file prepared by the author.